

A texture component model for predicting recrystallization textures

Myrjam Winning^{1, a}, Dierk Raabe^{1, b}, Abhijit Brahme^{1, c}

¹Max-Planck Institute for Iron Research GmbH, Depart. Microstructure Physics and Metal Forming,
Max-Planck Str.1, 40237 Düsseldorf, Germany

^am.winning@mpie.de, ^bd.raabe@mpie.de, ^ca.brahme@mpie.de

Keywords: recrystallization, simulation, steel, texture, anisotropy, Avrami, grain size, renormalization.

Abstract. The study presents an analytical model for predicting crystallographic textures and the final grain size during primary static recrystallization of metals using texture components. The kinetics is formulated as a tensorial variant of the Johnson-Mehl-Avrami-Kolmogorov (JMAK) equation. The tensor form is required since the kinetic and crystallographic evolution of the microstructure is described in terms of a limited set of growing (recrystallizing) and swept (deformed) texture components. The number of components required defines the order of the tensor since the kinetic coupling occurs between all recrystallizing and all deformed components. The new method is particularly developed for the fast and physically-based process simulation of recrystallization textures with respect to processing. The present paper introduces the method and applies it to the primary recrystallization of low carbon steels.

Introduction

Various models exist for predicting curvature-driven coarsening phenomena such as grain or subgrain growth and stored-energy driven transformations such as recrystallization. Typical approaches are JMAK methods, Ginzburg-Landau-type phase field models, cellular automata, Potts models, vertex models, or front tracking algorithms [1-7]. Only some of these methods are usually applied for predicting crystallographic textures. The most prominent ones in the texture community are the Potts model, cellular automata, and statistical JMAK models.

In this section a texture component based JMAK model will be introduced for the approximation of recrystallization textures. The approach is inspired by the Bunge-Köhler transformation approximation [8] and the Sebald-Gottstein microgrowth kinetic model [9,10].

The method is based on the representation of both, the deformation texture and the emerging recrystallization texture by a small set of discrete crystallographic Gauss-shaped texture components. These texture components are characterized in terms of their center orientation, volume fraction, and scatter in orientation space. The main idea of the approach consists in two aspects. Firstly, it reduces the number of deformed and newly formed recrystallized orientations to only a small number of discrete components. Secondly, it can make use of either a more physically-based renormalization scheme or of an empirical fitting procedure to average the required activation energies from pairs of single orientations into corresponding equivalent values which are valid for pairs of texture components.

The main idea of using a small set of texture components instead of a large set of discrete single orientations consists of course in reducing the computational time required for the prediction of recrystallization textures and kinetics. Another advantage of this method is that the approach offers a small set of parameters which can be fitted from experiments. Since each recrystallizing texture component can statistically interact with each deformation texture component the kinetics is formulated as a tensorial variant of the JMAK kinetic equation. Each element of the kinetic tensor is derived by a set of two differential equations. The first equation describes the thermally activated nucleation and growth processes among the deformed and recrystallizing texture components for the

expanded (unconstrained) volume fraction and the second equation is used for the correction to the true (constrained) volume fraction which accounts for impingement. The respective driving forces, nucleation energies, and mobility coefficients between all different couples, each consisting of a recrystallizing and a deformed component to be swept, can be obtained from renormalization or from fitting. The method provides a very fast and efficient way to phenomenologically predict recrystallization textures on the basis of a physically-based metallurgical approach.

The components which reproduce the deformation texture can be approximated from experimentally obtained pole figures or from single orientation data sets. A fixed set of texture components which may occur as potential nucleation components is then defined which can be fitted from known typical recrystallization textures for the material investigated. For instance in the case of rolled body centered cubic steels the most prominent potential recrystallization texture components are placed on or close to the $\langle 111 \rangle // \text{ND}$ texture fiber (ND: normal direction of the sheet) [11-16].

All nucleation texture components have the possibility to grow into all existing deformation texture components following their individual kinetics prescribed by the respective averaged activation energy for nucleation in a particular deformation component, the averaged mobility between the two components, and the driving force provided by the deformation component affected. The kinetic parameters are hence essentially defined by the activation energy for nucleation, the activation energy for grain boundary mobility, and the stored energy in the various deformation texture components relative to the various nucleation texture components that grow inside them. The kinetic parameters enter for each of the growing texture components, relative to the deformation components affected, a finite difference form of the JMAK kinetic equation under the assumption that the set of growing texture components sweeps the deformed texture components. The finite difference formulation has been earlier suggested by Sebald and Gottstein [9,10].

The model

First, it is assumed that all grains (deformed and recrystallized) are grouped into a small set of texture components one of which is a random component. This means that the models does not recognize grains but only groups of grains with similar orientation forming texture components. The number of discrete texture components typically required for instance for the case of low carbon steel sheets amounts to 5-10. A texture component is a spherical distribution function around a certain center orientation which is characterized by a scatter width in orientation space and a volume fraction in real space. The random texture component is equally spread throughout orientation space. The mathematical form of the components as used in this work will be introduced below.

Second, owing to the fact that the approach considers only a fixed set of components each with a certain specific orientation scatter, the activation energies for grain boundary mobility are no longer fixed constants but they must be obtained either from a suited renormalization or fitting procedure.

Third, as a consequence of the texture component approach the JMAK equation and the equation for the expanded volume assume a tensorial form. Each tensor element is in each time step defined by the kinetic equations for the expanded volume fraction and constrained volume fraction describing the growth of a recrystallizing component i into a deformation component j in difference form. One should underline that the indices i and j are in the following used to identify a certain texture component in the current texture but they do not indicate pairs of single orientations as for instance in the original version of this kind of model by Sebald and Gottstein [9,10].

Fourth, the driving force for the primary recrystallization is in each of the deformed texture components assumed to be constant and isotropic. The driving force associated with a specific deformation texture component depends on its center orientation and on the strain path history that it has experienced.

Under these conditions the difference for the expanded volume, $\Delta V_{ij}^{\text{exp}}$, can then be written

$$\Delta V_{ij}^{\text{exp}} = N_{ij} \frac{4}{3} \pi \left(\left(\langle r_{ij} \rangle + \langle \Delta r_{ij} \rangle \right)^3 - \langle r_{ij} \rangle^3 \right), \quad N_{ij} = \langle \dot{N}_{ij} \rangle \Delta t, \quad \langle \Delta r_{ij} \rangle = \langle v_{ij} \rangle \Delta t = \langle m_{ij} \rangle p_j \Delta t. \quad (1)$$

where the subscript ij indicates that the recrystallizing texture component i grows into the deformed texture component j . One should note that the summation rule which is commonly used for linear tensor operations does not apply in these equations. N_{ij} is the number of newly formed nuclei (formed during the preceding time interval) belonging to the recrystallizing texture component i growing within the deformation texture component j . $\langle \dot{N}_{ij} \rangle$ is the corresponding equivalent nucleation rate which may assume any form desired since it can be easily integrated in each time interval providing the number of fresh nuclei for the ensuing time step. The symbol $\langle r_{ij} \rangle$ indicates the equivalent radius of the recrystallizing texture component i (not that of a grain) growing within the deformation texture component j . $\langle \Delta r_{ij} \rangle$ indicates the increase of the equivalent radius of the recrystallizing texture component during the time step Δt and $\langle v_{ij} \rangle$ indicates the corresponding equivalent growth velocity of the texture component i (not of a grain) within the deformation texture component j . Inserting the driving forces provided by the j deformation texture components and the effective mobilities, $\langle m_{ij} \rangle$, between the i recrystallizing texture components and the j deformation texture components leads to the above given expression for $\langle \Delta r_{ij} \rangle$. The stored deformation energy per volume of the deformed component j , p_j , is a function of the deformed orientation component, of the total plastic strain, and of time so that the driving force is characteristic of the texture component and its deformation history. The time dependence is due to static recovery. In the current approach the recovery kinetics have been fitted from experimental hardness data obtained for low carbon steels [17].

The tensor equation introduced above is nonsymmetric, i.e. $\Delta V_{ij}^{\text{exp}} \neq \Delta V_{ji}^{\text{exp}}$. The symmetry is broken owing to the fact that the driving force which a recrystallizing component i experiences in a deformed component j is not the same as that which a recrystallizing component j experiences in a deformed component i . This absence of symmetry is general, i.e. it applies to both, single orientations and texture components. In contrast to that the mobility tensor may be assumed to be essentially symmetric among the texture components, i.e. $\langle m_{ij} \rangle = \langle m_{ji} \rangle$. This means that the grain boundary mobility of an equivalent crystal (i.e. of a texture component representing many single grains with similar orientations) i when growing into the deformed component j is the same (or at least very similar) as that of component j growing into component i .

Inserting the activation terms for the mobility and the nucleation rate tensors yields

$$N_{ij} = \dot{N}_{0ij} \left\langle \exp \left(- \frac{Q_{ij}^{\text{nuc}}}{k_B T} \right) \right\rangle \Delta t, \quad \langle \Delta r_{ij} \rangle = m_{0ij} \left\langle \exp \left(- \frac{Q_{ij}^{\text{mob}}}{k_B T} \right) \right\rangle p_j \Delta t. \quad (2)$$

where $\left\langle \exp \left(- \frac{Q_{ij}^{\text{mob}}}{k_B T} \right) \right\rangle$ is the thermal activation term of the grain boundary mobility for a texture component i that grows into the texture component j and $\left\langle \exp \left(- \frac{Q_{ij}^{\text{nuc}}}{k_B T} \right) \right\rangle$ is the thermal activation term for nucleation for a recrystallizing texture component i in a deformed texture component j . The activation energy matrix for the mobility is symmetric, $Q_{ij}^{\text{mob}} = Q_{ji}^{\text{mob}}$ while the energy matrix for nucleation is not symmetric, $Q_{ij}^{\text{nuc}} \neq Q_{ji}^{\text{nuc}}$.

The constrained volume for a heterogeneous solid in tensor notation

For tracking the kinetic evolution of the recrystallization texture in the course of a simulated heat treatment it is necessary that at each time step the following JMAK balance has to be calculated in order to correct the remaining deformation volume for the recrystallized fraction

$$\Delta V_{ij}^{RX} = X_j^{\text{def}} \Delta V_{ij}^{\text{exp}} . \quad (3)$$

where X_j^{def} is the remaining volume fraction of the deformed texture component j , ΔV_{ij}^{RX} the change in the true (constrained) volume of the expanding recrystallization component i during its growth into the deformed component j , and $\Delta V_{ij}^{\text{exp}}$ the expanded (unconstrained) volume of the expanding recrystallization component i during its growth into the deformed component j as derived in the preceding section.

The remaining volume fraction X_j^{def} is calculated by the initial volume fraction of this component before the start of the heat treatment, X_{0j}^{def} , minus the sum of all recrystallizing texture components, $n=1$ to $n=n_{\text{max}}$, which have already swept some portion of the deformation texture component j , $\sum_{n=1}^{n_{\text{max}}} X_{nj}^{RX}$. This leads to

$$\Delta V_{ij}^{RX} = \left(X_{0j}^{\text{def}} - \sum_{n=1}^{n_{\text{max}}} X_{nj}^{RX} \right) \Delta V_{ij}^{\text{exp}} . \quad (4)$$

The two sets (unconstrained volume, constrained volume) of coupled $i \times j$ difference equation systems described by the equations above can be solved by an explicit finite difference scheme for all possible pairs of recrystallizing and deformed texture components. The actual selection of suited texture components must be conducted on the basis of the chosen deformation starting texture data (low carbon sheet steels in the current study) from which the deformation texture components can be fitted [11-16]. The fitting can be conducted using well established standard methods [18-20].

Some experience in the field of recrystallization texture development is required for using the model since in the current formulation a certain set of possible recrystallization texture components from which the texture emerges must be prescribed. The actual selection, though, which component grows and which does not grow is then simulated according to the kinetics outlined above. It should be noted at this point that the formulations derived above exactly reproduce the Sebal-Gottstein model for recrystallization when applied to large sets of pairs of single discrete orientations [9,10] rather than to small sets of pairs of texture components.

The starting point for the renormalization procedure is the approach that all the expanding crystals which belong to the same orientation component can be replaced by one single equivalent expanding sphere which then represents a large set of single grains with similar orientation in the further treatment. The same argumentation applies for the decomposition of the deformation texture where the deformed crystals are summarized into an equivalent set of texture components which are gradually swept by the recrystallizing components.

The model functions used in this work for fitting crystallographic textures have been discussed in [18-20]. They have an individual orientation density and full width at half maximum as a measure for the strength and scatter of the texture component they represent. They are used here in the form of central functions, i.e. their orientation scatter is isotropic.

The half width of the texture components obtained from the texture component fit which has to be conducted prior to the actual recrystallization simulation enters the model by influencing the activation energy for recrystallization nucleation via an empirical function. This procedure reflects the common observation that texture components of ferritic steels which typically have a large

internal orientation gradient (orientation scatter) a more prone to undergo nucleation events than texture components which have a very homogeneous orientation without large gradients after cold rolling [21-23,17]. The newly recrystallizing texture components have all the same half width in the current model.

Example of the simulation of texture and grain size evolution during primary static recrystallization of a low carbon steel sheet

In this section the new JMAK model will be applied to the prediction of recrystallization textures of a low carbon sheet steel. The deformation components were reproduced from an experimentally determined cold rolling texture. A fixed set of further texture components which typically occurs as potential nucleation and recrystallization components was then defined according to experimental experience. The actual selection which of those potential recrystallization texture components finally prevail evolves during the simulation owing to the kinetic evolution equations and by the renormalized (or fitted) model parameters. For instance in the case of rolled low carbon body centered cubic steels the most prominent potential recrystallization texture components are located in the vicinity of the $\langle 111 \rangle // \text{ND}$ texture fiber [11-16]. All recrystallization texture components are in principle admitted to grow into all of the existing deformation texture components following their individual kinetics for nucleation, mobility, and driving force in each of the different deformation components.

The kinetic parameters are essentially defined by the activation energy for nucleation of a recrystallization component i in a deformation component j ; the renormalized activation energy of the grain boundary mobility among these two components, and the stored deformation energy in the various deformation texture components.

Input data and parameters for the recrystallization simulation

The deformation texture of an 80% cold rolled low carbon steel sheet was fitted from experimental data [11] using the texture component method in the version of Helming et al. [18-20]. In principle also any other decomposition method providing a set of discrete texture components could be used for this first step of the procedure. The texture fit was conducted in a way to minimize the number of used components (6 deformation components including a random component) in order to perform a very fast recrystallization simulation. It is also possible to increase the number of components for higher precision. The texture components for the current example are given in table 1.

The driving force data for the individual texture components were obtained by fitting the corresponding integral of the stress-strain behavior of the cold rolled low carbon steel sheet for different cold rolling reductions and by varying this value through the Taylor factor of each individual component, table 1.

The data for the activation energy of the grain boundary mobility were simply fitted to match typical experimental observations. The few data that were used in this study from experiments stem from the work of Gottstein et al. [24-27]. Missing data were set as adjustable parameters and fitted to experimentally observed recrystallization textures. In the model essentially three types of grain boundaries have been used, namely, low angle grain boundaries which have a low mobility, high angle grain boundaries which have a larger mobility, and one type of special grain boundary ($27^\circ \langle 110 \rangle$) with a very high mobility. The activation energy data for the nucleation rates within the different deformed texture components were fitted by coupling them to the deformation energy and the orientation scatter width of the individual deformed texture components. Components with a high driving force and large orientation scatter had the smallest activation energy for nucleation.

The assumed annealing temperature amounted to 900 K so that the material remains during heat treatment in the ferritic regime (intercritical annealing strategies are not yet considered at this stage). The grain size of the starting material was 35 μm . The final average grain size after completed primary static recrystallization can be tracked during the simulation by using the equation

$$d_{ij} = d \exp\left(-\frac{Q_{ij}^{\text{nuc}} - Q_{ij}^{\text{mob}}}{4 k_B T}\right) \quad (5)$$

where d_{ij} is the average grain size the grains belonging to the recrystallizing texture component i growing within the deformed texture component j and d is the grain size prior to recrystallization. Grain shape aspects are not yet considered in this study.

ϕ_1 [°]	ϕ [°]	ϕ_2 [°]	Miller indices {hkl}<uvw>	full width at half maximum [°]	Taylor- factor [1]	Driving force [MPa]	volume fraction after deformation [vol.%]
30.0	54.7	45.0	{111}<112>	12.0	3.5	4.1232	10.0
0.0	54.7	45.0	{111}<110>	12.0	3.2	3.7698	15.0
0.0	0.0	45.0	{001}<110>	12.0	2.6	3.0629	12.0
0.0	35.0	45.0	{112}<110>	12.0	3.0	3.5341	24.0
0.0	25.2	45.0	{113}<110>	12.0	2.8	3.2985	29.0
0.0	45.0	0.0	{011}<100>	20.0	3.7	4.3588	0.0
Random texture component						3.8876	10.0

Table 1 Deformation texture components used for the current simulation.

Simulation results and discussion

Fig. 1 shows the orientation distribution functions (ODF) after cold rolling and after the simulated recrystallization (20 s, 900 K).

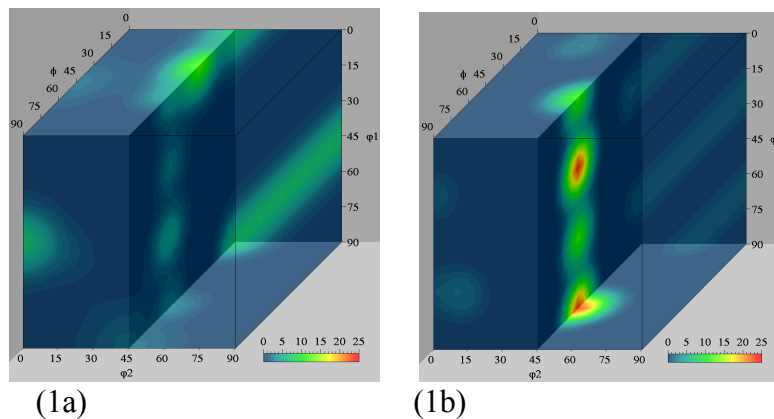
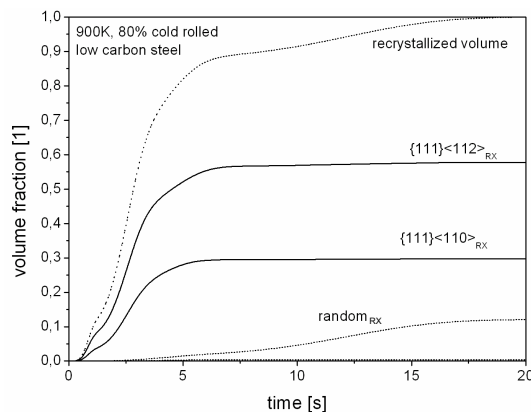


Fig. 1 (a) Crystallographic texture after cold rolling obtained from component decomposition of an experimental cold rolling texture (80% cold rolled, low carbon steel); (b) texture after simulated recrystallization (20 s, 900 K). The units are in multiples of random orientation density.

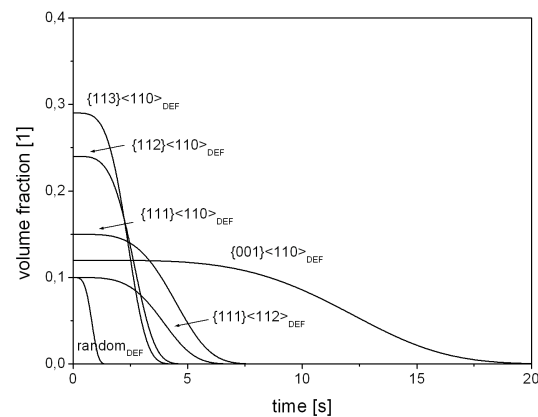
According to the bcc crystal symmetry and the approximated orthotropic symmetry of the cold rolling process defined by rolling direction, normal direction, and transverse direction of the sheets the textures are presented in the reduced Euler space ($0^\circ \leq \phi_1, \phi, \phi_2 \leq 90^\circ$) [28]. Since ferritic steels tend to develop pronounced texture fibers during cold rolling [11,12,17,21], it is convenient to present the ODF in the form of a $\phi_2 = 45^\circ$ section as shown in Fig. 1 revealing two characteristic orientation fibers, namely, the α_{bcc} -fiber (fiber axis <110> parallel to the rolling direction including major components {001}<110>, {112}<110>, and {111}<110>) and the γ -fiber (fiber axis <111> parallel to the normal direction including major components {111}<110> and {111}<112>). Both

ODFs are scaled to a maximum orientation density of $f(g)=25$. While the starting texture was dominated by the well known α_{bcc} -fiber texture the recrystallization produces a γ -fiber.

Fig. 2 shows the predicted kinetic evolution of the main texture components. The index RX indicates the volume fraction of the recrystallized texture component. The data show, that the material has undergone complete primary static recrystallization after about 20s, i.e. the recrystallized volume amounts to 100% by practical means. Counting only the two main γ -fiber texture components $\{111\}\langle 110\rangle$ and $\{111\}\langle 112\rangle$ the recrystallization is even complete after about 5s. The kinetics reveals that only these two main orientations play a role for the overall kinetic evolution. This prediction is in accordance with the common observation of texture evolution in that field [11,12].



(2)



(3)

Fig. 2 Simulation at 900K on the basis of the cold rolling texture shown in Fig. 1. The index RX indicates the volume fraction of the respective texture component which is newly developed during primary static recrystallization.

Fig. 3 Simulation at 900K on the basis of the cold rolling texture shown in Fig. 1. The index DEF indicates the volume fraction of the texture components in the deformed microstructure.

Fig. 3 shows for the same simulation (900K) the gradual drop of the main deformation texture components, namely, for the $\{001\}\langle 110\rangle$, $\{113\}\langle 110\rangle$, $\{112\}\langle 110\rangle$, $\{111\}\langle 110\rangle$ and $\{111\}\langle 112\rangle$ components. It must be noted that the $\{111\}\langle 110\rangle$ and the $\{111\}\langle 112\rangle$ components occur both as deformation texture components and as recrystallization texture components. The $\{001\}\langle 110\rangle$ texture component has the slowest kinetics while the $\{113\}\langle 110\rangle$ and the $\{112\}\langle 110\rangle$ components are swept very fast during recrystallization.

This effect of reluctant recrystallization in some texture components (for instance, in $\{001\}\langle 110\rangle$) and very high recrystallization nucleation rates (for instance in $\{112\}\langle 110\rangle$) has been well documented in the literature on the textures of bcc steels and other bcc metals [11–17,21–23]. In these earlier studies which were mostly conducted on low carbon steels it was reported that the kinetics of recrystallization and the resulting grain morphology may considerably depend on the grain orientation of the deformed grain. In $\{001\}\langle 110\rangle$ oriented grains recrystallization can be substantially delayed in the case of a small and even entirely be suppressed in the case of a large grain size. In $\{112\}\langle 110\rangle$ oriented grains both recrystallization and recovery were observed in the literature. However, nucleation in these grains was never observed to be entirely suppressed as observed in $\{001\}\langle 110\rangle$ oriented crystals. The smallest activation energy for nucleation was associated with $\{111\}\langle uvw\rangle$ oriented crystals which are typically among the first grains to recrystallize [12]. A more detailed discussion of the recrystallization behavior of $\{111\}\langle uvw\rangle$ and $\{112\}\langle 110\rangle$ oriented grains has already been the subject of numerous studies in the past [11–17,21–23]. In these investigations it was mostly suggested that the strong tendency of $\{111\}$ oriented grains to produce high nucleation rates can be attributed first to the small cell sizes, i.e. to

the high dislocation densities stored in them, and second to the formation of microstructural inhomogeneities such as shear bands which provide strong local misorientations within these grains.

Summary

A new model for predicting recrystallization textures and the final grain size was introduced. It is a tensorial variant of the kinetic JMAK approach formulating the kinetic evolution of recrystallization in terms of a fixed small set of growing (recrystallizing) and swept (deformed) texture components. The method was applied to a simple problem of recrystallization of a low carbon steel sheet.

References

- [1] F.J. Humphreys: *Materials Sc. and Tech.* 8 (1992), p. 135.
- [2] A.D. Rollett: *Progress in Mater. Sc.* 42 (1997), p. 79.
- [3] D. Raabe: *Computational Materials Science* (Wiley-VCH, Weinheim, 1998).
- [4] O. Engler and H.E. Vatne: *JOM* 50 (1998), p. 23.
- [5] D. Raabe: *Adv. Eng. Mater.* 3 (2001), p. 745.
- [6] E.A. Holm and C.C. Battaile: *JOM* 9 (2000), p. 20.
- [7] D. Raabe, F. Roters, F. Barlat and L.Q. Chen (Eds.): *Continuum Scale Simulation of Engineering Materials* (Wiley-VCH, Weinheim, 2004).
- [8] H.J. Bunge and U. Köhler: *Scripta Metall.* 27 (1992), p. 1539.
- [9] R. Sebald and G. Gottstein: *Acta Mater.* 50 (2002), p. 1587.
- [10] R. Sebald and G. Gottstein: in *Proc. ICOTOM 12*, 1 (1999), p. 292.
- [11] M. Hölscher, D. Raabe and K. Lücke: *Steel Research* 62 (1991), p. 567.
- [12] W.B. Hutchinson: *Int. Mat. Rev.* 29 (1984), p. 25.
- [13] D. Raabe and K. Lücke: *Materials Sci. & Tech.* 9 (1993), p. 302.
- [14] C. Klinkenberg, D. Raabe and K. Lücke: *Steel Research* 63 (1992), p. 227.
- [15] D. Raabe: *Steel Research* 66 (1995), p. 222.
- [16] P. Juntunen, D. Raabe, P. Karjalainen, T. Kopio and G. Bolle: *Metall. Mater. Trans. A* 32 (2001), p.1989.
- [17] D. Raabe: *Scripta Metall.* 33 (1995), p. 735.
- [18] D. Raabe and F. Roters: *Intern. J. Plasticity* 20 (2004), p. 339.
- [19] K. Lücke, J. Pospiech, J. Jura and J. Hirsch: *Z. Metallkunde* 77 (1986), p. 312.
- [20] K. Helming, R.A. Schwarzer, B. Rauschenbach, S. Geier, B. Leiss, H. Wenk, K. Ullemeier and J. Heinitz: *Z. Metallkunde* 85 (1994), p. 545.
- [21] C. Därmann, S. Mishra and K. Lücke: *Acta Metall.* 32 (1984), p. 2185.
- [22] U. von Schlippenbach, F. Emren and K. Lücke: *Acta Metall.* 34 (1986), p. 1289.
- [23] D. Raabe, Z. Zhao, S.J. Park and F. Roters: *Acta Mater.* 50 (2002), p. 421.
- [24] G. Gottstein and L.S. Shvindlerman: *Grain Boundary Migration in Metals - Thermodynamics, Kinetics, Applications* (CRC Press, Boca Raton, 1999).
- [25] G. Gottstein, V. Marx and R. Sebald: in *Recrystallization and Related Phenomena*, T. Sakai, H.G. Suzuki (Eds.), The Japan Inst. of Metals, 1999, p. 15.
- [26] L.S. Shvindlerman and G. Gottstein: in *Recrystallization and Related Phenomena*, T. Sakai, H.G. Suzuki (Eds.), The Japan Inst. of Metals, 1999, p. 431.
- [27] M. Furtkamp, G. Gottstein, D.A. Molodov, V.N. Semenov and L.S. Shvindlerman: *Acta Mater.* 46 (1998), p. 4103.
- [28] H.J. Bunge: *Texture analysis in materials science* (Butterworths, London, 1982).